

## Accepted Manuscript

Sessile droplet contact angle of water–Al<sub>2</sub>O<sub>3</sub>, water–TiO<sub>2</sub> and water–Cu nanofluids

Janusz T. Cieśliński, Katarzyna A. Krygier

PII: S0894-1777(14)00145-9

DOI: <http://dx.doi.org/10.1016/j.expthermflusci.2014.06.004>

Reference: ETF 8240

To appear in: *Experimental Thermal and Fluid Science*

Received Date: 2 December 2013

Revised Date: 30 May 2014

Accepted Date: 3 June 2014

Please cite this article as: J.T. Cieśliński, K.A. Krygier, Sessile droplet contact angle of water–Al<sub>2</sub>O<sub>3</sub>, water–TiO<sub>2</sub> and water–Cu nanofluids, *Experimental Thermal and Fluid Science* (2014), doi: <http://dx.doi.org/10.1016/j.expthermflusci.2014.06.004>

This is a PDF file of an unedited manuscript that has been accepted for publication. As a service to our customers we are providing this early version of the manuscript. The manuscript will undergo copyediting, typesetting, and review of the resulting proof before it is published in its final form. Please note that during the production process errors may be discovered which could affect the content, and all legal disclaimers that apply to the journal pertain.



**Sessile droplet contact angle of water-Al<sub>2</sub>O<sub>3</sub>, water-TiO<sub>2</sub> and water-Cu nanofluids**

Janusz T. Cieśliński<sup>a\*</sup> and Katarzyna A. Krygier<sup>b</sup>

Gdańsk University of Technology, Gdansk, 80-233, Poland

<sup>a</sup>jcieslin@pg.gda.pl, <sup>b</sup>krygier.kasia@gmail.com

\*Corresponding author: Tel:+48 58 347-16-22 Fax:+48 58 347-13-83

E-mail address: [jcieslin@pg.gda.pl](mailto:jcieslin@pg.gda.pl)

**Abstract**

This work presents measurements of the contact angle of sessile droplets for three nanofluids, i.e. water-Al<sub>2</sub>O<sub>3</sub>, water-TiO<sub>2</sub> and water-Cu. The plates made of glass, anodized aluminium and stainless steel of different roughness served as substrates. Ultrasonic vibration was used for 30-60 minutes in order to stabilise the dispersion of the nanoparticles. Nanoparticles were tested at the concentration of 0.01%, 0.1%, and 1% by weight. Three methods of contact angle measurement were applied. The contact angle was established directly by use of a KRÜSS DSA10 goniometer or - building on digital images of droplets, an appropriate geometrical approach and tangent methods were applied. The study revealed that the droplet contact angle of nanofluids depends on surface roughness, type of substrate, material of nanoparticles, and concentration of nanoparticles.

**Keywords:** Contact angle, Nanofluids, Roughness

**Nomenclature:**

D – diameter



DIA – droplet image approach

DIG – droplet geometrical approach

G – goniometer

h – height

r – radius

$\alpha$  - contact angle

## 1. Introduction

Due to enhanced thermophysical properties, nanofluids can find application in many cooling/heating systems [1,2]. Therefore, it is of great importance to precisely establish such properties of nanofluids as thermal conductivity, viscosity and parameters particularly influencing boiling heat transfer, i.e. surface tension and contact angle. It has been postulated that the major reason of critical heat flux improvement in nanofluids is the decrease of static contact angle due to nanocoating formation on the heating surface, and by definition, the liquid wets a surface more when the contact angle is smaller. The nanocoating – formed on surface during boiling process of nanofluid, could significantly enhance the surface wettability [3]. Very limited data regarding contact angle of nanofluids are available in the open literature [4-11]. Wasan and Nikolov [4] using video microscopy technique, observed improved spreading of nanofluids due to ordering of nanoparticles near the liquid/solid contact line. As nanoparticles latex spheres of 1  $\mu\text{m}$  in diameter were used. Chengara et al. [5] discussed the role of the structural disjoining pressure exerted by nanoparticles on the spreading of a liquid film containing these particles. Vafaei et al. [6] established that addition of even small amount of (BiTe) nanoparticles dramatically changes the wetting characteristics. For pure water the contact angle was very small and increased beyond 40° for the nanoparticle concentration of  $3 \cdot 10^{-6}$  grams of BiTe nanoparticles per gram of deionised



water. Kim et al. [7] determined that droplet contact angle of water-ZrO<sub>2</sub> nanofluid practically does not depend on the nanoparticle concentration and is the same as for water (79°). Jeong et al. [8] fixed that water-Al<sub>2</sub>O<sub>3</sub> nanofluid with nanoparticle concentration of 0.5%, 1%, 2% and 4% by volume show very small contact angle on quenched surfaces (5°-15°). Kim et al. [7], Coursey and Kim [9] and Golubovic et al. [10] postulated that the major reason of critical heat flux improvement in nanofluids is the decrease of static contact angle due to nanocoating formation on the heating surface. Kim et al. [7] proposed the modified Young's equation for the contact angle estimation of nanoparticle-fouled surfaces. Sefiane et al. [11] building on advancing/receding contact line analysis determined, that the nanoparticles in the vicinity of the triple line enhance dynamic wetting behaviour of the ethanol-Al nanofluids for concentrations up to ~1% by weight. Vafaei and Wen [12] established that the presence of gold nanoparticles significantly affects gas bubble dynamics such as the triple line and the instantaneous contact angle. Particularly, promotion of the pinning behaviour of the bubble triple line was identified due to presence of 5 nm gold nanoparticles.

The objective of this work was to investigate the effect of nanoparticle concentration and substrate state on the static droplet contact angle. The surface state was characterized by three roughness parameters. The plates made of glass, anodized aluminium and stainless steel served as a substrate. In each series of measurements fresh nanofluids were used to generate sessile droplets. Alumina (Al<sub>2</sub>O<sub>3</sub>) and titania (TiO<sub>2</sub>) oxides were tried mainly for ease of manufacture and stabilization compared to pure metallic particles (Cu), which are difficult to suspend without agglomeration. Water was selected as a base fluid because of potential application of the tested fluids in water heating systems.

## **2. Experimental facility and procedure**

### ***2.1. Experimental setup and procedure***



Two experimental stands were used to measure droplet contact angle, namely KRÜSS DSA10 goniometer – Fig. 1 and in-house developed test stand – Fig. 2. Droplets of known volume of 2 $\mu$ L were deposited on a substrate using an automatic dispenser or was injected slowly onto the solid surface by a syringe. The experiments were conducted under similar air conditioned laboratory environments. In order to eliminate the impact of droplet evaporation on the measured values of the contact angle, the images of the droplets were taken directly after their deposition – no later than 1 minute.

## 2.2. Contact angle measurement

Values of the contact angle were determined by use of a goniometer (G) or from captured image of a droplet. Building on the digital images of the droplets geometrical approach (DIG) and developed tangent method (DIA) were applied. Depending on the level of wettability two formulas were used in geometrical approach. For contact angles lower than 30° relationship (1):

$$\operatorname{tg} \alpha = \frac{2h}{d} \quad (1)$$

was applied [13,14], while for contact angles higher than 30°, formula (2):

$$\cos \alpha = \frac{r^2 - h^2}{r^2 + h^2} \quad (2)$$

was used [15], where r and h are radius and height of the droplet, respectively – Fig. 3.

The tangent method (DIA) is based on the following algorithm:

1. choose points along the droplet/air interface and one on the heater surface – Fig. 4,
2. fit an ellipse through the points on the droplet/air interface,
3. calculate the tangent at the intersection between this ellipse and the horizontal,
4. determine the contact angle from the inverse tangent.

For both approaches average the contact angle was calculated as an arithmetic mean for 10



droplets, and for each droplet three measurements were done as a rule. As an example Fig. 5 illustrates the distribution of contact angle values of ten water-TiO<sub>2</sub>(1%) droplets deposited on the stainless steel substrate. In this case geometrical approach - using Eq. 2, was applied to determine the contact angles. It seems, that scatter of the data was mainly caused by manual deposition of the droplets.

### 2.3. Error analysis

According to producer of the KRÜSS DSA10 goniometer resolution of the contact angle measurement is 0.1°.

The uncertainties of the calculated contact angle values based on digital images were estimated using the mean-square method. The experimental uncertainty of the contact angle lower than 30° (Eq. 1) was estimated as follows:

$$\Delta(\operatorname{tg} \alpha) = \sqrt{\left(\frac{\partial(\operatorname{tg} \alpha)}{\partial d} \Delta d\right)^2 + \left(\frac{\partial(\operatorname{tg} \alpha)}{\partial h} \Delta h\right)^2} \quad (3)$$

where the absolute maximal measurement errors of the diameter  $\Delta d$  and height  $\Delta h$  of the droplet are 0.1 mm and 0.1 mm, respectively. The experimental uncertainty of the contact angle higher than 30° (Eq. 2) was estimated from the expression:

$$\Delta(\cos \alpha) = \sqrt{\left(\frac{\partial(\cos \alpha)}{\partial r} \Delta r\right)^2 + \left(\frac{\partial(\cos \alpha)}{\partial h} \Delta h\right)^2} \quad (4)$$

where the absolute maximal measurement errors of the radius and height  $\Delta h$  of the droplet are 0.1 mm and 0.1 mm, respectively. So, the uncertainties of the calculated contact angle values based on the digital images (geometrical approach) were equal to  $\pm 1^\circ$ .

The mean-square method was used also, to estimate the uncertainty of the tangent method. Assuming that only two first steps (mentioned above) contribute to the uncertainty in the contact angle estimation, the absolute measurement error reads:



$$\Delta(\text{tg}\alpha) = \sqrt{[\Delta(\text{tg}\alpha)_{\text{coord}}]^2 + [\Delta(\text{tg}\alpha)_{\text{fit}}]^2} \quad (5)$$

where  $\Delta(\text{tg}\alpha)_{\text{coord}}$  is the absolute error that results from the designation of the coordinates of the chosen points along the droplet/air interface and  $\Delta(\text{tg}\alpha)_{\text{fit}}$  is the absolute error that results from the fit of an ellipse through the points on the droplet/air interface. For small angles  $\text{tg}\alpha \approx \alpha$ , and the absolute errors  $\Delta(\text{tg}\alpha)_{\text{coord}}$  and  $\Delta(\text{tg}\alpha)_{\text{fit}}$  are equal to the measurement errors of the length and can be assumed as 0.05 mm and 0.05 mm, respectively. So, the uncertainties of the calculated contact angle values based on tangent method were equal to  $\pm 4^\circ$ .

#### **2.4. Preparation and characterization of nanofluids**

In the present study  $\text{Al}_2\text{O}_3$ ,  $\text{TiO}_2$  and Cu were used as nanoparticles while distilled, deionized water was applied as a base fluid. Alumina ( $\text{Al}_2\text{O}_3$ ) nanoparticles, of spherical form had a diameter ranging from 5 nm to 250 nm; their mean diameter was estimated to be 47 nm according to the manufacturer (Sigma-Aldrich Co.). Titania ( $\text{TiO}_2$ ) nanoparticles, of spherical form had a diameter ranging from 5 nm to 250 nm; their mean diameter was estimated to be 47 nm according to the manufacturer. Copper nanoparticles, of spherical form had diameter from 7 nm to 257 nm; their mean diameter was estimated to be 48 nm according to the manufacturer. Dispersants were not used to stabilise the suspension. Ultrasonic vibration was used for 30-60 minutes in order to stabilise the dispersion of the nanoparticles. Nanoparticles were tested at the concentration of 0.01%, 0.1%, and 1% by weight. The pH of nanofluids was about 7. The stability of the produced water- $\text{Al}_2\text{O}_3$ , water- $\text{TiO}_2$  nanofluids was pretty good, which means they could stay for a few days without visually observable sedimentation, while for water-Cu nanofluid the segregation time was of



the order of hours.

### **2.5. Characteristics of substrates**

The contact angles of the tested nanofluids were measured on plates made of glass, anodized aluminium and stainless steel (316L). The stainless steel plates were roughed with emery paper 360, 500, 1000 and 2000. The surfaces of the substrates were cleaned after each of test series with acetone and dried in air freely. The roughness parameters of the tested surfaces were determined by use of the profile measurement gauge Hommel Tester T500 with vertical and horizontal resolutions equal to 20 nm and 40 nm, respectively. The measured roughness parameters of the tested substrates are shown in Tab. 1. The roughness profile of one of the tested stainless steel plates (Fig. 6), shows that the surface was smooth and homogeneous.

## **3. Results**

As an example Fig. 7 displays photographs of the sessile droplets of nanofluid water-Cu on the stainless steel substrate. The photographs were obtained by use of the goniometer. It is seen in Fig. 7 that the increase in nanoparticle concentration results in contact angle decrease.

Fig. 8, in turn, illustrates photographs of the sessile droplets of nanofluid water- $\text{Al}_2\text{O}_3$  and water-Cu on the stainless steel substrate. The nanoparticle concentration was the same and equal to 1%. The photographs were obtained by use of the goniometer. As results from Fig. 8a, contact angle of water- $\text{Al}_2\text{O}_3$  nanofluid droplet is greater than for water-Cu droplet, so it means that water-Cu nanofluid exhibits better wettability than water- $\text{Al}_2\text{O}_3$  nanofluid (Fig. 8b).

### **3.1. Influence of nanoparticle concentration**



Fig. 9 illustrates the influence of nanoparticle concentration (0.01%, 0.1%, and 1% by weight) on the droplet contact angle of water- $\text{Al}_2\text{O}_3$  nanofluid on the stainless steel substrate of different roughness. Contact angle was measured by use of KRÜSS DSA10 goniometer. It is seen in Fig. 9 that addition of even small amount of alumina nanoparticles results in dramatic increase in contact angle. This phenomenon indicates that the nanoparticles really affect the force balance in the vicinity of the triple line and as a result wetting behaviour of the nanofluids. Furthermore, alike as in [6] the non-monotonic variation of contact angle with nanoparticle concentration was observed. According to Vafaei et al. [6] possible explanation of this phenomenon are the particle-fluid interactions and low range electrostatic interactions between the nanoparticles that depend on nanoparticle concentration and size.

It is worthy to stress that contact angle for pure water measured in present study almost does not depend on roughness like in [16], and contrary to the results published in [17], where contact angle of pure water decreases with the increase of roughness. However, in [17] the contact angle measurements were carried out in the environment of pure water vapor.

Present results for pure water – for given roughness  $R_a=0.1 \mu\text{m}$  and by use of the same measuring instrument - KRÜSS DSA10 goniometer, are in excellent agreement with data obtained in [7] - point 1 in Fig. 7.

### ***3.2. Influence of the substrate***

Fig. 10 illustrates the influence of the substrate, i.e. glass, anodized aluminium and stainless steel versus nanoparticle concentration on droplet contact angle of water- $\text{TiO}_2$  nanofluid.

Contact angles were measured using KRÜSS DSA10 goniometer. It is of interest that droplet contact angle for distilled water on stainless steel and anodized aluminium is practically the same -  $79^\circ$  and  $80^\circ$ , respectively and distinctly smaller for glass -  $22^\circ$ . Moreover, droplet contact angle of water-TiO<sub>2</sub> nanofluid on stainless steel substrate almost does not depend on nanoparticle concentration while for glass increases almost monotonically with nanoparticle concentration increase. Droplet contact angle for anodized aluminium substantially increased for the highest nanoparticle concentration tested, i.e. 1%. The impact of the substrate on contact angle results from complex molecular, electrostatic and chemical interactions between the material of the surface, nanoparticles and liquid molecules near the triple line. The emanation of these interactions are surface forces and one of the important manifestation of these forces is the disjoining pressure [5,11]. A more detailed study on the surface structure and surface forces is needed to further explain the influence of the substrate on contact angle.

### ***3.3. Influence of nanoparticle material***

Fig. 11 displays the influence of the type of nanoparticle material (Al<sub>2</sub>O<sub>3</sub>, TiO<sub>2</sub> and Cu) versus nanoparticle concentration on droplet contact angle of water-based nanofluids on the stainless steel substrate. It is seen in Fig. 11, that independent of tested nanoparticle materials and nanoparticle loading, addition of nanoparticles results in increase of contact angle compared to pure water. This clearly demonstrates the vital impact of nanoparticles on the force balance at the contact line. Contact angle reaches maximum and minimum for water-TiO<sub>2</sub> nanofluid at nanoparticle concentration of 0.01% and 0.1%, respectively. Contrary to present data, values of contact angle for water-Al<sub>2</sub>O<sub>3</sub> nanofluid obtained in [7] decrease with



nanoparticle concentration increase. This discrepancy may result from different geometry of the substrate, i.e. thin wire in [7] and flat plate in present study, different roughness of the substrate, that is not given in [7], and various volume of the droplets – 5  $\mu\text{L}$  and 2  $\mu\text{L}$ , in [7] and present study, respectively.

### **3.4. Influence of surface roughness**

Fig. 12 shows the influence of stainless steel substrate roughness on the contact angle of the three tested nanofluids at the same nanoparticle concentration, i.e. 1%. Contact angles were measured using KRÜSS DSA10 goniometer. It seems that droplet contact angle of water-Cu nanofluid decreases with roughness increase, while for water-TiO<sub>2</sub> and water-Al<sub>2</sub>O<sub>3</sub> nanofluids substantially increases with roughness increase. As it was discussed in [18] the wetting characteristics of rough surfaces depends on the relationship between the droplet size and the scale of the roughness. In the case of nanofluids another factor may affect the contact angle of rough surfaces, namely the ratio of the mean roughness to the nanoparticle diameter  $R_d/D_p$ . For large values of this ratio, i.e. for relatively rough surfaces, the nanoparticles may settle in the cavities thereby affecting its mouth size and cavity angle.

### **3.5. Evaluation of measurement methods**

Fig. 13 shows comparison of the results of contact angle measurements of water-Cu nanofluid droplets on glass. As it is seen in Fig. 13 droplet contact angle of water-Cu nanofluid obtained by three applied methods displays the same tendency of increase/decrease of contact angle versus nanoparticle concentration. Furthermore, the discrepancy between measurements made by use of KRÜSS DSA10 goniometer and based on digital images is distinctly lower for nanofluids than for distilled water.

## **4. Conclusions**

The study revealed that the droplet contact angle of nanofluids depends on roughness, type of substrate, material of nanoparticles, and concentration of nanoparticles.

The droplet contact angle for distilled water on stainless steel and anodized aluminium is practically the same and distinctly smaller than for the glass substrate.

The droplet contact angle of water-Cu nanofluid on stainless steel and glass substrates almost does not depend on the nanoparticle concentration.

## References

- [1] K.V. Wong, O. De Leon, Applications of Nanofluids: Current and Future, Hindawi Publishing Corporation Advances in Mechanical Engineering, (2010) Article ID 519659, <http://dx.doi.org/10.1155/2010/519659>
- [2] R. Saidur, K.Y. Leong, H.A. Mohammad, Review on applications and challenges of nanofluids, Renewable and Sustainable Energy Reviews, Vol. 15 (2011) 1646–1668.
- [3] S.L. Song et al., CHF enhancement of SiC nanofluid in pool boiling experiment, Exp. Therm. Fluid Sci. (2013), <http://dx.doi.org/10.1016/j.expthermflusci.2013.08.008>
- [4] D.T. Wasan, A.D. Nikolov, Spreading of nanofluids on solids. Nature, Vol. 423 (2003) 156-159.
- [5] A. Chengara, A.D. Nikolov, D.T. Wasan, A. Trokhymchuk, D. Henderson, Spreading of nanofluids driven by the structural disjoining pressure gradient. J. Colloid Interface Sc., Vol. 280 (2004) 192–201.
- [6] S. Vafaei, T. Borca-Tasciuc, M.Z. Podowski, A. Purkayastha, G. Ramanath, P.M. Ajayan, Effect of nanoparticles on sessile droplet contact angle, Nanotechnology, Vol. 17, no. 10, (2006) 2523–2527.
- [7] S.J. Kim, I.C. Bang, J. Buongiorno, L.W. Hu, Surface wettability change during pool boiling of nanofluids and its effect on critical heat flux. Int. J. Heat Mass Transfer, Vol. 50, (2007) 4105-4116.
- [8] Y.H. Jeong, W.J. Chang, S.H. Chang, Wettability of heated surfaces under pool boiling using surfactant solutions and nano-fluids. Int. J. Heat Mass Transfer, Vol. 51, (2008) 3025–



3031.

[9] J.S. Coursey, J. Kim, Nanofluid boiling: The effect of surface wettability. *Int. J. Heat Fluid Flow*, Vol. 29, (2008) 1577-1585.

[10] M.N. Golubovic, H.D. Madhawa Hettiarachchi, W.M. Worek, W.J. Minkowycz, Nanofluids and critical heat flux, experimental and analytical study. *Applied Thermal Engineering*, Vol. 29, (2009) 1281–1288.

[11] K. Sefiane, J. Skilling, J. MacGillivray, Contact line motion and dynamic wetting of nanofluid solutions. *Advances in Colloid and Interface Science*, Vol. 138, (2008) 101–120.

[12] S. Vafaei, D. Wen, Bubble formation in a quiescent pool of gold nanoparticle suspension, *Advances in Colloid and Interface Science*, Vol. 159 (2010) 72–93.

[13] A.W. Adamson, *Physical Chemistry of Surfaces*, 5<sup>th</sup> ed. New York: Wiley InterScience, Wiley&Sons, Inc. (1990)

[14] E.T. Dutkiewicz, *Physical Chemistry of Surfaces*, Warsaw: WNT, (1998) (in Polish).

[15] P. Zielke, J. Szymczyk, A. Delgado, Bestimmung kritischer Radien von Tropfen auf Oberflächen mit einem Gradienten der Benetzbarkeit. *PAMM*, Vol. 8, (2008) 10651-10652.

[16] L. Boulangé-Petermann, J. Rault, M.-N. Bellon-Fontaine, Adhesion of streptococcus thermophilus to stainless steel with different surface topography and roughness, *Biofouling*, Vol. 11(3) (1997) 201-216.

[17] S.G. Kandlikar, M.E. Steinke, Contact angles and interface behavior during rapid evaporation of liquid on a heated surface, *Int. J. of Heat and Mass Transfer*, Vol. 45 (2002) 3771–3780.

[18] G. Wolansky Marmur A., Apparent contact angles on rough surfaces: the Wenzel equation revisited, *Colloids and Surfaces*, Vol. 156 (1999) pp. 381-388.



**Figure captions**

Fig. 1. Krüss DSA10 goniometer

Fig. 2. Scheme of the test rig: 1 – digital camera, 2 - substrate, 3 - droplet, 4 - screen, 5 – light source

Fig. 3. Droplet profile

Fig. 4. Curve fit and tangent determination

Fig. 5. Contact angle values of ten water-TiO<sub>2</sub>(1%) droplets

Fig. 6. Roughness profile of the stainless steel plate ( $R_a = 0.03 \mu\text{m}$ )

Fig. 7. Influence of nanoparticle concentration: a) 0.01%, b) 1% on contact angle of nanofluid water-Cu on stainless steel substrate ( $R_a=0.18 \mu\text{m}$ )

Fig. 8. Droplet contact angle of: a) water-Al<sub>2</sub>O<sub>3</sub> and b) water-Cu nanofluids on stainless steel substrate ( $R_a=0.18 \mu\text{m}$ ); nanoparticle concentration – 1%

Fig. 9. Droplet contact angle of water-Al<sub>2</sub>O<sub>3</sub> nanofluid on stainless steel substrate

Fig. 10. Static contact angle of water-TiO<sub>2</sub> nanofluid on glass, aluminium and stainless steel substrate

Fig. 11. Droplet contact angle of water-Al<sub>2</sub>O<sub>3</sub>, water-Cu and water-TiO<sub>2</sub> nanofluids on stainless steel substrate ( $R_a=0.12 \mu\text{m}$ )

Fig. 12. Droplet contact angle of water-Al<sub>2</sub>O<sub>3</sub>, water-Cu and water-TiO<sub>2</sub> nanofluids on stainless steel substrate of different roughness

Fig. 13. Static contact angle of water-Cu nanofluid droplets on glass substrate

Tab. 1. Roughness parameters of the tested substrates

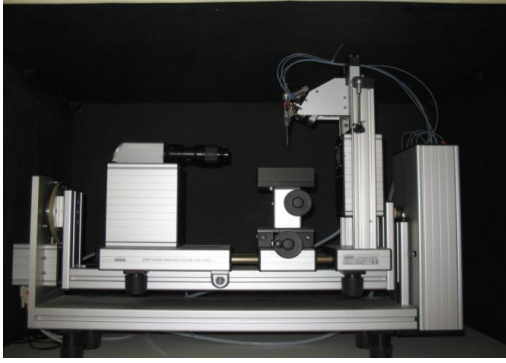
Substrate	$R_a$ [ $\mu\text{m}$ ]	$R_z$ [ $\mu\text{m}$ ]	$W_a$ [ $\mu\text{m}$ ]
Glass	0.02	0.093	0,023
Stainless steel	0.03	0.263	0,023
	0.04	0.397	0,043
	0.12	1.54	0,04
	0.18	1.72	0,073

$R_a$  - an average arithmetical roughness in the range of sampling length

$R_z$  - an arithmetic average of absolute height of five the highest roughness' peaks and height of five the deepest valleys in the range of sampling length

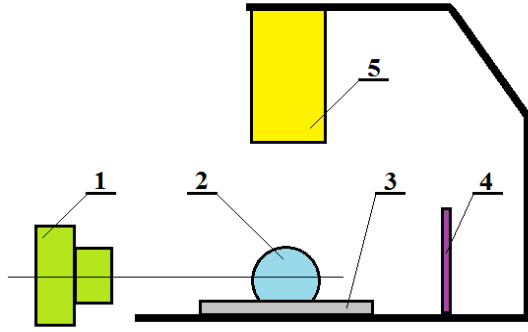
$W_a$  - arithmetical mean deviation in the range of sampling length



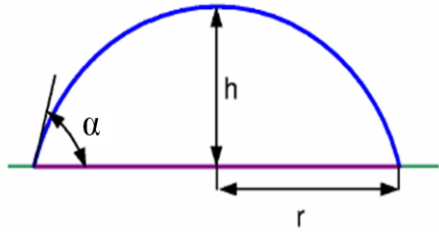


ACCEPTED MANUSCRIPT

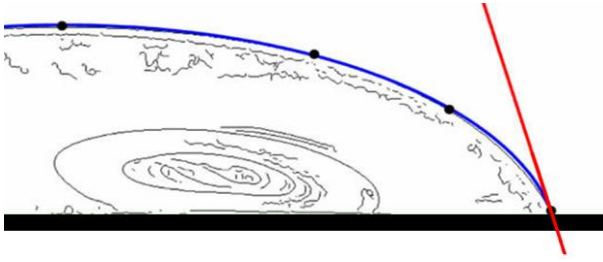




ACCEPTED MANUSCRIPT

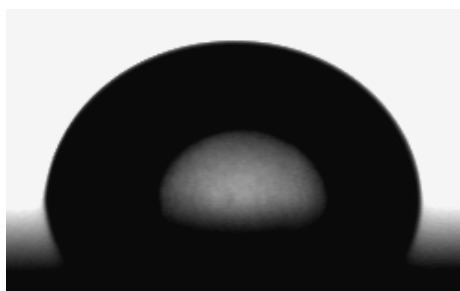


ACCEPTED MANUSCRIPT

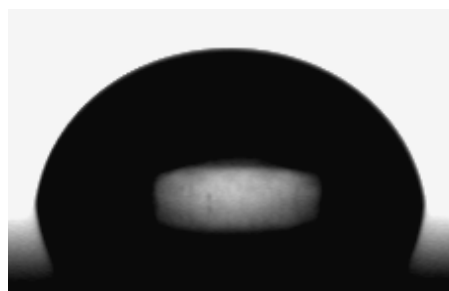


ACCEPTED MANUSCRIPT

a)

 $\alpha=91.5^\circ$ 

b)

 $\alpha=85.1^\circ$ 

ACCEPTED MANUSCRIPT

a)



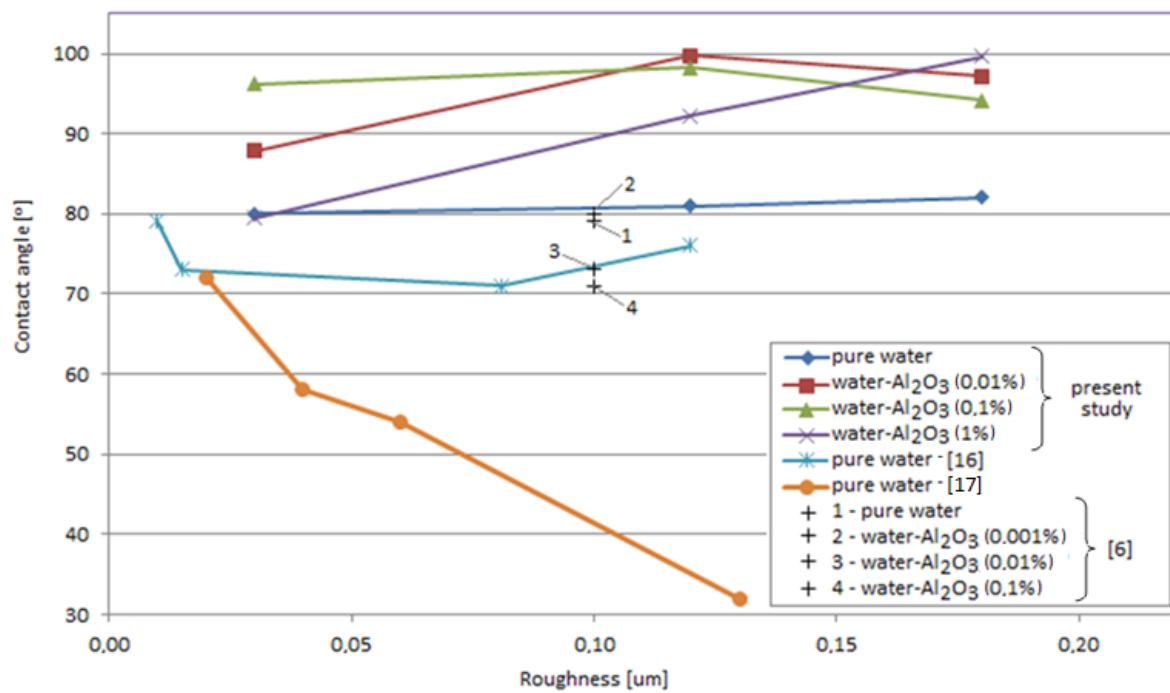
$$\alpha=89.6^{\circ}$$

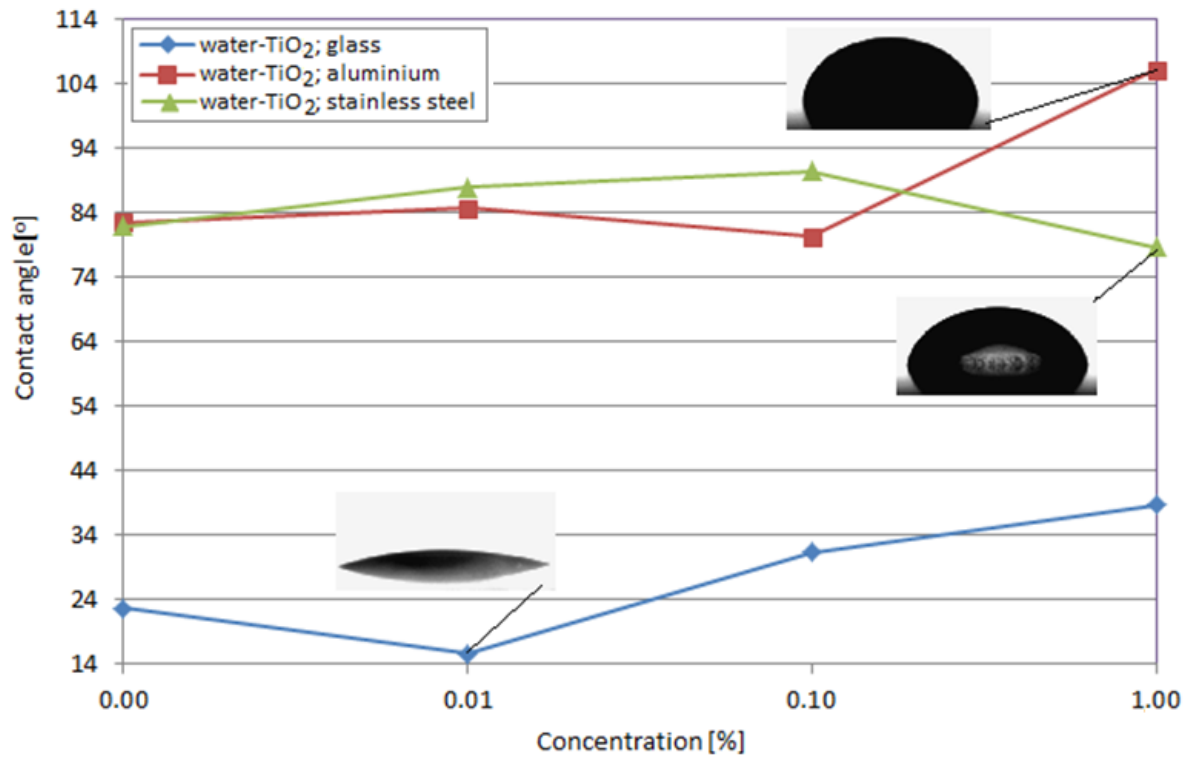
b)

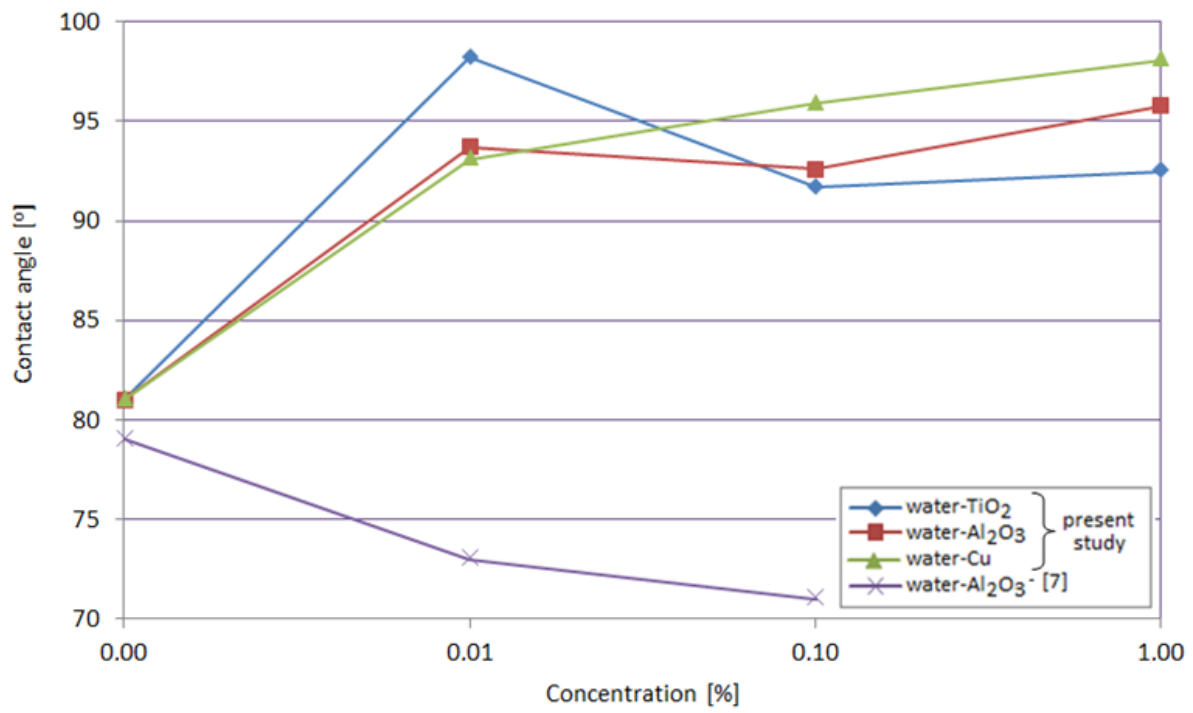


$$\alpha=91.5^{\circ}$$

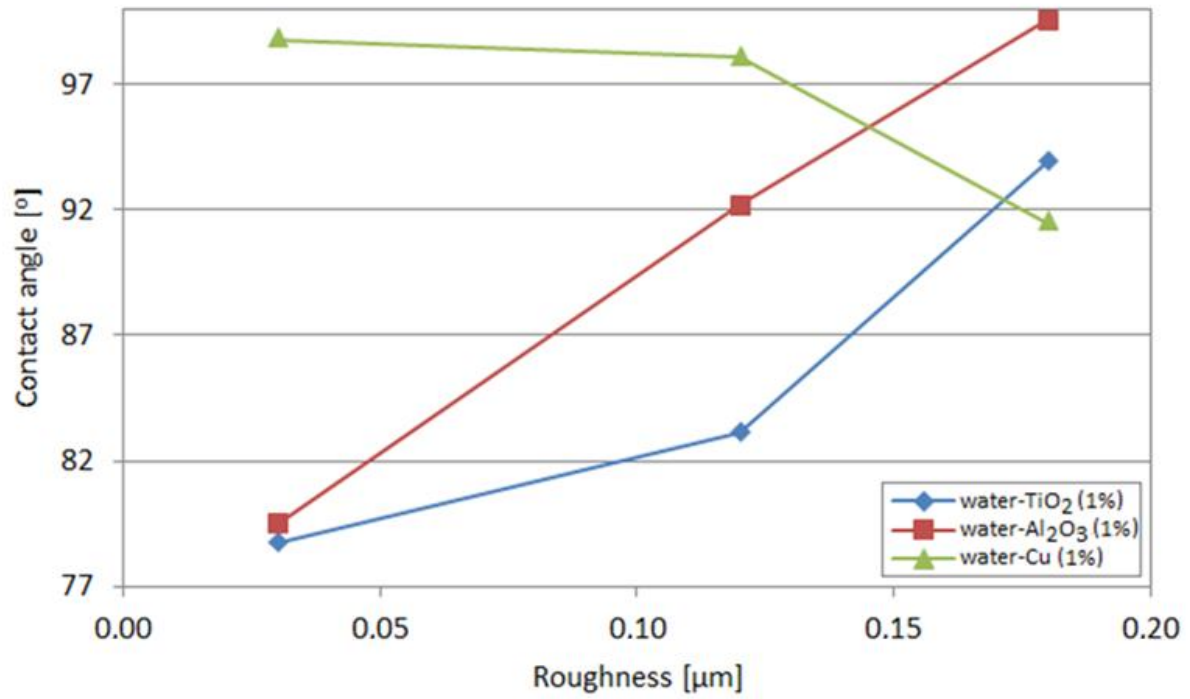
ACCEPTED MANUSCRIPT

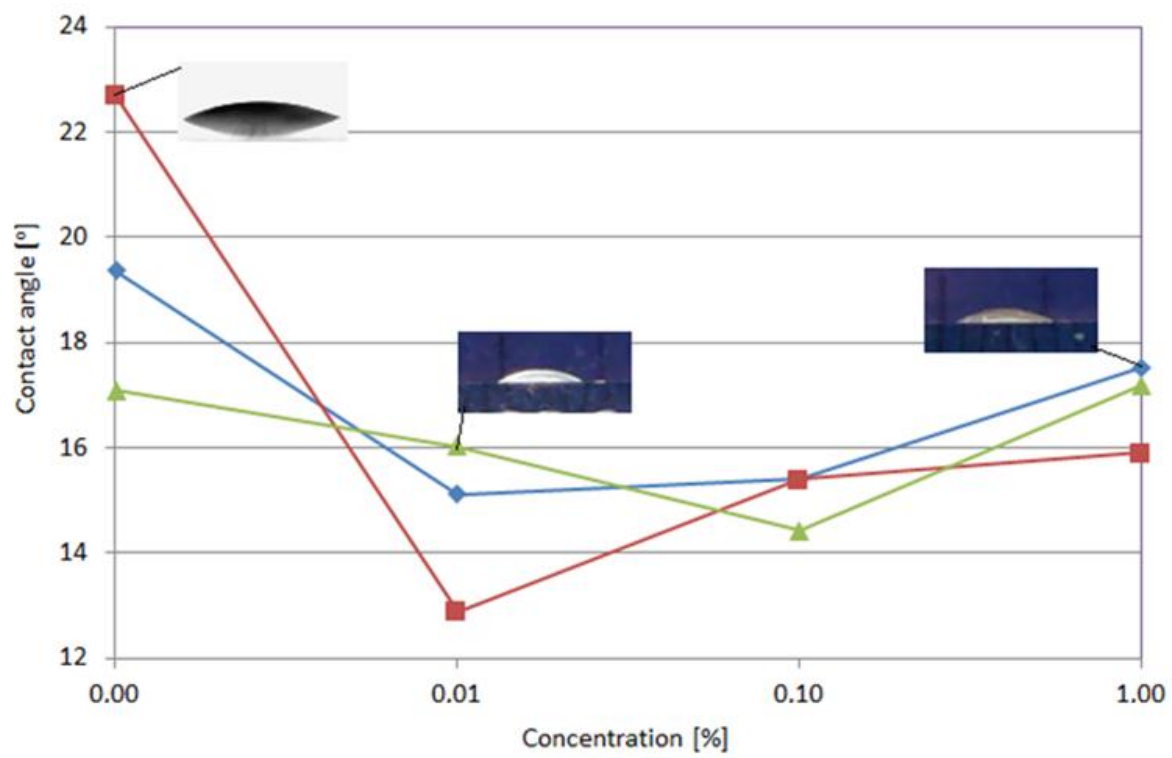












**Research highlights**

- 1- Static contact angle of sessile droplets of three nanofluids has been measured
- 2- Influence of nanoparticle type and concentration has been revealed.
- 3- Influence of substrate type and roughness has been established.
- 4- Three methods of contact angle determination have been applied.

ACCEPTED MANUSCRIPT